FRUCD Model Handbook

A collection of nomenclature, equations, and sources for the models implemented in FRUCD vehicle simulations.

Editors:
Blake Christierson (2018-2021)
Leonardo Howard (2020-)
Tristan Pham (2020-)
Sam Kilduff (2020-)

Formula Racing at UC Davis
Mechanical & Aerospace Department
University of California, Davis
April 2022

Contents

Chapter 1

Introduction

This document serves as living documentation for all of the models present in the FRUCD vehicle simulation platform. To start, the first chapter establishes conventions that are used throughout the various models of systems that comprise the vehicle. This covers widely used nomenclature, formatting guidelines, and the definition of standard coordinate systems.

1.1 Formatting Guidelines

1.1.1 Typesetting Conventions

1.1.2 Coding Conventions

1.2 Nomenclature

The nomenclature is separated into several different types of which the definitions are stated below:

- Inputs: Functions supplied to a model that it will react to.
- Outputs: The data series characterizing the response of the system to the given input. These are also most likely states.
- Variables: These represent the degrees of freedom (DoFs) of the system or model being studied.
- Parameters: The constants or lookup functions that are being designed to better the performance of a system
- Constants: Universal constants that hold true across all design conditions

1.3 Coordinate Systems

FRUCD adheres to the z-up SAE coordinate system as described by SAE-J670-2008. This section will outline several of the important coordinate systems that comprise the overall system and their relative transformations and uses.

Before discussing the various important coordinate systems, some basics about coordinate systems and navigating between them must be established. Moving between coordinate systems requires a combination of translations and rotations that when composed are called a rigid frame transformation. The standard method for rotation is a sequence of rotation matrices corresponding with a z-y-x rotation sequence. This corresponds with the SAE-J670-2008 definition of the yaw (ψ), pitch (θ), and roll (ϕ) vehicle body Euler angles. Note that in some kinematic frames the order of rotation will differ due to certain angles having static constant angles and other being dynamic degrees of freedom (DoFs). In this case, the static set of z, y, and/or x rotations are applied first followed by the dynamic rotations. Below are examples of rotation matrices about each principle axis of a frame:

$$R_x^{F_1 \to F_2}(\theta_x) := \begin{bmatrix} 1 & 0 & 0 \\ 0 & \cos\theta_x & -\sin\theta_x \\ 0 & \sin\theta_x & \cos\theta_x \end{bmatrix} \tag{1.3.1}$$

$$R_y^{F_1 \to F_2}(\theta_y) := \begin{bmatrix} \cos\theta_y & 0 & \sin\theta_y \\ 0 & 1 & 0 \\ -\sin\theta_y & 0 & \cos\theta_y \end{bmatrix} \tag{1.3.2}$$

$$R_z^{F_1 \to F_2}(\theta_z) := \begin{bmatrix} \cos\theta_z & -\sin\theta_z & 0 \\ \sin\theta_z & \cos\theta_z & 0 \\ 0 & 0 & 1 \end{bmatrix} \tag{1.3.3}$$

$$R^{F_1 \to F_2}(\boldsymbol{\theta}) := R_x^{F_1 \to F_2}(\theta_x) \cdot R_y^{F_1 \to F_2}(\theta_y) \cdot R_z^{F_1 \to F_2}(\theta_z) \tag{1.3.4}$$

Note that the rotations are applied via matrix multiplication and therefore appear right to left in the complete rotation matrix equation for the full sequence. By first applying a translation to the position in the original frame we can transform any coordinate to any other coordinate in 3D space using the previously defined rotation convention:

$$O^{F_1 \to F_2}(\mathbf{x}_0) := (x, y, z) = \mathbf{x}_0 \tag{1.3.5}$$

$$T^{F_1 \to F_2}(\mathbf{x}_0, \boldsymbol{\theta}) : F_1 \ni \mathbf{p} \longrightarrow \mathbf{p}' := R^{F_1 \to F_2}(\boldsymbol{\theta}) \cdot (\mathbf{p} - \mathbf{x}_0) \in F_2 \tag{1.3.6}$$

This provides a definition for the standard coordinate transformation; however, as will be detailed in the next sections, specific transformations may slightly differ.

1.3.1 Earth-Fixed (World) Coordinate System: X-Y-Z (E)

The earth-fixed or world coordinate system serves as an inertial reference for all of the other frames. Per the z-up SAE system the Z axis is aligned with the gravitational vector and oriented upwards out of the ground plane. The X and Y axes are arbitrarily oriented and placed in the ground plane in SAE-J670-2008. For all FRUCD simulations, the X-Y origin is defined as the intersection of the racing line and the start line. The X axis is aligned with the direction of the racing line at this intersection. Lastly, the Y axis is defined to follow the right hand rule between the now defined X and Z axes.

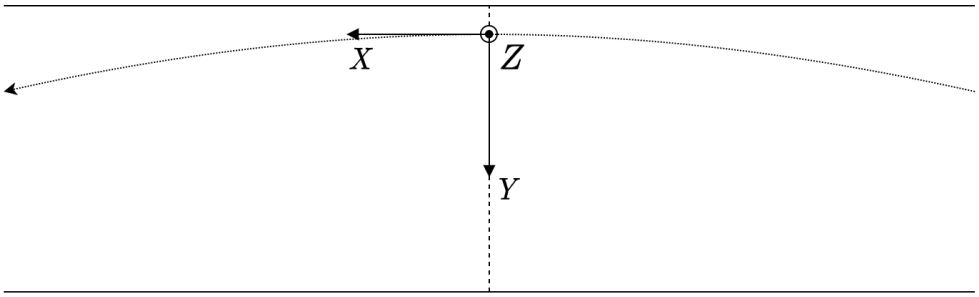

Figure 1.1: Earth-Fixed (World) Coordinate System Definition

1.3.2 Intermediate Coordinate System: x-y-z (I)

The intermediate coordinate system travels parallel to the ground plane underneath the center of gravity of the vehicle. This defines a global displacement vector and the yaw angle of the vehicle. The z axis is parallel to the Z axis of the world coordinate system while the x axis is aligned with the heading of the vehicle. The yaw angle, ψ describes the rotation of the intermediate coordinate system relative to the world coordinate system.

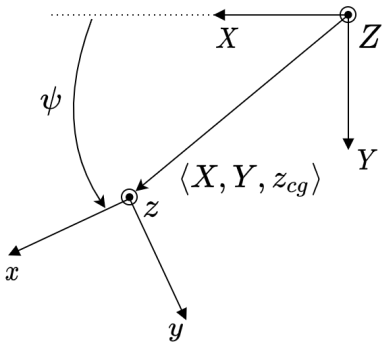

Figure 1.2: Intermediate Coordinate System Definition

The coordinate

1.3.3 Body (Sprung) Coordinate System: x_B-y_B-z_B (B)

1.3.4 Aerodynamic Coordinate System: x_A-y_A-z_A (A)

1.3.5 Axle Coordinate System: x_X-y_X-z_X (X)

1.3.6 Tire Coordinate System: x_T-y_T-z_T (T)

1.3.7 Wheel Coordinate System: x_W-y_W-z_W (W)

Chapter 2

Chassis Dynamics

2.1 Planar Dynamics Models

2.1.1 3-DOF Bicycle Model

Symbol	Unit	Type	Description
$x, \dot{x}, \ddot{x}$	m, $\frac{m}{s}$, $\frac{m}{s^2}$	Output	Longitudinal States
$y, \dot{y}, \ddot{y}$	m, $\frac{m}{s}$, $\frac{m}{s^2}$	Output	Lateral States
$\psi, \dot{\psi}, \ddot{\psi}$	rad, $\frac{rad}{s}$, $\frac{rad}{s^2}$	Output	Yaw States
m	kg	Parameter	Unsprung Mass
I_{zz}	$kg - m^2$	Parameter	Unsprung Yaw Inertia
δ	deg	Input	Steer Angle
${}_T F_{(x\|y),(f\|r)}$	N	Input	Tire Forces

Table 2.1: 3-DOF Bicycle Model Nomenclature

$$m(\ddot{x} - \dot{y}\dot{\psi}) = F_{x,f}\cos\delta - F_{y,f}\sin\delta + F_{x,r} \tag{2.1.1}$$
$$m(\ddot{y} + \dot{x}\dot{\psi}) = F_{y,f}\cos\delta + F_{x,f}\sin\delta + F_{y,r} \tag{2.1.2}$$
$$I_{zz}\ddot{\psi} = a\left(F_{y,f}\cos\delta + F_{x,f}\sin\delta\right) - bF_{y,r} \tag{2.1.3}$$

$$\ddot{x} = \frac{1}{m}\left[F_{x,f}\cos\delta - F_{y,f}\sin\delta + F_{x,r}\right] + \dot{y}\dot{\psi} \tag{2.1.4}$$
$$\ddot{y} = \frac{1}{m}\left[F_{y,f}\cos\delta + F_{x,f}\sin\delta + F_{y,r}\right] - \dot{x}\dot{\psi} \tag{2.1.5}$$
$$\ddot{\psi} = \frac{1}{I_{zz}}\left[a\left(F_{y,f}\cos\delta + F_{x,f}\sin\delta\right) - bF_{y,r}\right] \tag{2.1.6}$$

2.1.2 3-DOF Full-Track Model

Symbol	Unit	Type	Description
$x, \dot{x}, \ddot{x}$	$m, \frac{m}{s}, \frac{m}{s^2}$	Output	Longitudinal States
$y, \dot{y}, \ddot{y}$	$m, \frac{m}{s}, \frac{m}{s^2}$	Output	Lateral States
$\psi, \dot{\psi}, \ddot{\psi}$	$rad, \frac{rad}{s}, \frac{rad}{s^2}$	Output	Yaw States
m_s	kg	Parameter	Sprung Mass
$m_{u,(f\|r)}$	kg	Parameter	Front & Rear Unsprung Mass
$I_{zz,u}$	$kg - m^2$	Parameter	Unsprung Yaw Inertia
$\%F$	$[\,]$	Parameter	Front Weight Distribution
δ_i	deg	Input	Steer Angle
${}_TF_{(x\|y),i}$	N	Input	Tire Forces

Table 2.2: 3-DOF Full-Track Model Nomenclature

$$m(\ddot{x} - \dot{y}\dot{\psi}) = F_{x,1}\cos\delta_1 + F_{x,2}\cos\delta_2 - F_{y,1}\sin\delta_1 - F_{y,2}\sin\delta_2 \tag{2.1.7}$$

$$m(\ddot{y} + \dot{x}\dot{\psi}) = F_{y,1}\cos\delta_1 + F_{x,1}\sin\delta_1 + F_{y,2}\cos\delta_2 + F_{x,2}\sin\delta_2 + F_{y,3} + F_{y,4} \tag{2.1.8}$$

$$I_{zz}\ddot{\psi} = a\left(F_{y,1}\cos\delta_1 + F_{x,1}\sin\delta_1 + F_{y,2}\cos\delta_2 + F_{x,2}\sin\delta_2\right) - b(F_{y,3} + F_{y,4}) \tag{2.1.9}$$

$$\ddot{x} = \frac{1}{m}(F_{x,1}\cos\delta_1 + F_{x,2}\cos\delta_2 - F_{y,1}\sin\delta_1 - F_{y,2}\sin\delta_2) + \dot{y}\dot{\psi} \tag{2.1.10}$$

$$\ddot{y} = \frac{1}{m}(F_{y,1}\cos\delta_1 + F_{x,1}\sin\delta_1 + F_{y,2}\cos\delta_2 + F_{x,2}\sin\delta_2 + F_{y,3} + F_{y,4}) - \dot{x}\dot{\psi} \tag{2.1.11}$$

$$\ddot{\psi} = \frac{1}{I_{zz}}(a\left(F_{y,1}\cos\delta_1 + F_{x,1}\sin\delta_1 + F_{y,2}\cos\delta_2 + F_{x,2}\sin\delta_2\right) - b(F_{y,3} + F_{y,4})) \tag{2.1.12}$$

2.2 Vertical & Attitude Dynamics Models

2.2.1 2-DOF Quarter Car Model

Symbol	Unit	Type	Description
$z_s, \dot{z_s}, \ddot{z_s}$	$m, \frac{m}{s}, \frac{m}{s^2}$	Output	Vertical States of Sprung Mass
$z_u, \dot{z_u}, \ddot{z_u}$	$m, \frac{m}{s}, \frac{m}{s^2}$	Output	Vertical States of Unsprung Mass
k_s	$\frac{N}{m}$	Parameter	Suspension Spring Stiffness
k_t	$\frac{N}{m}$	Parameter	Tire Stiffness
m_s	kg	Parameter	Sprung Mass
m_u	kg	Parameter	Unsprung Mass
b_s	$\frac{Ns}{m}$	Parameter	Damping Coefficient
z_r	m	Input	Road Surface Displacement

Table 2.3: 2-DOF Quarter Car Model

$$\ddot{z_u} = \frac{k_s(z_s - z_u) + b_s(\dot{z_s} - \dot{z_u}) - k_t(z_u - z_r)}{m_u} \tag{2.2.1}$$

$$\ddot{z_s} = \frac{-k_s(z_s - z_u) - b_s(\dot{z_s} - \dot{z_u})}{m_s} \tag{2.2.2}$$

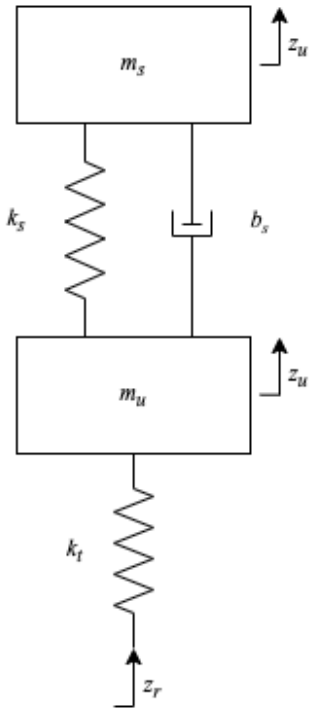

Figure 2.1: 2 DOF Quarter Car Model Diagram

2.2.2 4-DOF Half Car Model

Symbol	Unit	Type	Description
$x, \dot{x}, \ddot{x}$	m, $\frac{m}{s}$, $\frac{m}{s^2}$	Output	Longitudinal States
$z_s, \dot{z_s}, \ddot{z_s}$	m, $\frac{m}{s}$, $\frac{m}{s^2}$	Output	Vertical States of Sprung Mass
$z_{u_{,(r\|f\|L\|R)}}, \dot{z_u}_{,(r\|f\|L\|R)}, \ddot{z_u}_{,(r\|f\|L\|R)}$	m, $\frac{m}{s}$, $\frac{m}{s^2}$	Output	Vertical States of Unsprung Mass
$\theta, \dot{\theta}, \ddot{\theta}$	rad, $\frac{rad}{s}$, $\frac{rad}{s^2}$	Output	Pitch States
$k_{s_{,(r\|f\|L\|R)}}$	$\frac{N}{m}$	Parameter	Suspension Spring Stiffness
$k_{t_{,(r\|f\|L\|R)}}$	$\frac{N}{m}$	Parameter	Tire Stiffness
m_s	kg	Parameter	Sprung Mass
$m_{u_{,(r\|f\|L\|R)}}$	kg	Parameter	Unsprung Mass
$c_{s_{,(r\|f\|L\|R)}}$	$\frac{Ns}{m}$	Parameter	Damping Coefficient
$I_{yy,s}$	$kg - m^2$	Parameter	Sprung Pitch Inertia
t_w	m	Parameter	Track Width
$z_{(r\|f\|L\|R)}, \dot{z}_{(r\|f\|L\|R)}$	m, $\frac{m}{s}$	Input	Road

Table 2.4: 4-DOF Half Car Model

$$\left(m_s + m_{uf} + m_{ur}\right)\ddot{x} = \sum_{i=1}^{4} F_{x,i} \tag{2.2.3}$$

$$F_{z,(3+4)}b - F_{z,(1+2)}a - \left(m_s + m_{uf} + m_{ur}\right)\ddot{x}z_s = 0 \tag{2.2.4}$$

$$\begin{aligned} m_s\ddot{z_s} = &-k_{s,f}\left(z_s - a\theta - z_{u,f}\right) - k_{s,r}\left(z_s + b\theta - z_{u,r}\right) \\ &- c_{s,f}\left(\dot{z}_s - a\dot{\theta} - \dot{z}_{u,f}\right) - c_{s,r}\left(\dot{z}_s + b\dot{\theta} - \dot{z}_{u,r}\right) - m_s g \end{aligned} \tag{2.2.5}$$

$$\begin{aligned} I_{yy,s}\ddot{\theta} = &-k_{s,f}(-a)\left(z_s - a\theta - z_{u,f}\right) - k_{s,r}b\left(z_s + b\theta - z_{u,r}\right) \\ &- c_{s,f}(-a)\left(\dot{z}_s - a\dot{\theta} - \dot{z}_{u,f}\right) - c_{s,r}b\left(\dot{z}_s + b\dot{\theta} - \dot{z}_{u,r}\right) \end{aligned} \tag{2.2.6}$$

$$\begin{aligned} m_{u,f}\ddot{z}_{u,f} = &-k_{s,f}\left(z_{u,f} - z_s + a\theta\right) - c_{s,f}\left(\dot{z}_{u,f} - \dot{z} + a\dot{\theta}\right) \\ &+ k_{t,f}\left(z_{r,f} - z_{u,f}\right) + F_{z,(1+2)} - m_{u,f}g \end{aligned} \tag{2.2.7}$$

$$\begin{aligned} m_{u,r}\ddot{z}_{u,r} = &-k_{s,r}\left(z_{u,r} - z_s - b\theta\right) - c_{s,r}\left(\dot{z}_{u,r} - \dot{z} - b\dot{\theta}\right) \\ &+ k_{t,r}\left(z_{r,r} - z_{u,r}\right) + F_{z,(3+4)} - m_{u,r}g \end{aligned} \tag{2.2.8}$$

$$(m_s + m_{uf} + m_{ur})\,\ddot{y} = \sum_{i=1}^{4} F_{y,i} \tag{2.2.9}$$

$$F_{z,(1+3)}\frac{t_w}{2} - F_{z,(2+4)}\frac{t_w}{2} - (m_s + m_{uf} + m_{ur})\,\ddot{y} z_s = 0 \tag{2.2.10}$$

$$\begin{aligned} m_s\ddot{z}_s = &-k_{s,R}\left(z_s - \frac{t_w}{2}\theta - z_{u,R}\right) - k_{s,L}\left(z_s + \frac{t_w}{2}\theta - z_{u,L}\right) \\ &-c_{s,R}\left(\dot{z}_s - \frac{t_w}{2}\dot{\theta} - \dot{z}_{u,R}\right) - c_{s,L}\left(\dot{z}_s + \frac{t_w}{2}\dot{\theta} - \dot{z}_{u,L}\right) - m_s g \end{aligned} \tag{2.2.11}$$

$$\begin{aligned} I_{yy,s}\ddot{\theta} = &-k_{s,R}(-\frac{t_w}{2})\left(z_s - \frac{t_w}{2}\theta - z_{u,R}\right) - k_{s,L}\frac{t_w}{2}\left(z_s + \frac{t_w}{2}\theta - z_{u,L}\right) \\ &-c_{s,f}(-\frac{t_w}{2})\left(\dot{z}_s - \frac{t_w}{2}\dot{\theta} - \dot{z}_{u,R}\right) - c_{s,L}\frac{t_w}{2}\left(\dot{z}_s + \frac{t_w}{2}\dot{\theta} - \dot{z}_{u,L}\right) \end{aligned} \tag{2.2.12}$$

$$\begin{aligned} m_{u,R}\ddot{z}_{u,R} = &-k_{s,R}\left(z_{u,R} - z_s + \frac{t_w}{2}\theta\right) - c_{s,R}\left(\dot{z}_{u,R} - \dot{z} + \frac{t_w}{2}\dot{\theta}\right) \\ &+k_{t,R}\left(z_{r,R} - z_{u,R}\right) + F_{z,(1+3)} - m_{u,R}g \end{aligned} \tag{2.2.13}$$

$$\begin{aligned} m_{u,L}\ddot{z}_{u,L} = &-k_{s,L}\left(z_{u,L} - z_s - \frac{t_w}{2}\theta\right) - c_{s,L}\left(\dot{z}_{u,L} - \dot{z} - \frac{t_w}{2}\dot{\theta}\right) \\ &+k_{t,L}\left(z_{r,L} - z_{u,L}\right) + F_{z,(2+4)} - m_{u,L}g \end{aligned} \tag{2.2.14}$$

2.3 Comprehensive Dynamics Models

2.3.1 5-DOF Sampo Model

Symbol	Unit	Type	Description
$\Delta F_{z(F/R)}$	N	Output	Normal Load Transfer
$d_{s(F/R)}$	m	Parameter	Distance (COG of ms to roll axis)
$h_{u(F/R)}$	m	Parameter	Height of Unsprung Mass CG
$h_{s(F/R)}$	m	Parameter	Height of Sprung Mass CG
k_C	$\frac{Nm}{deg}$	Parameter	Chassis Torsional Stiffness
$k_{(F/R)}$	$\frac{Nm}{deg}$	Parameter	Front and Rear Roll Stiffness
$m_{s(F/R)}$	kg	Parameter	Sprung Mass
$m_{u(F/R)}$	kg	Parameter	Unsprung Mass
$t_{(F/R)}$	m	Parameter	Track Width
$z_{(F/R)}$	m	Parameter	Roll Center Height
a_y	$\frac{m}{s^2}$	Input	Vehicle Lateral Acceleration

Table 2.5: 5-DOF Sampo Model Nomenclature

$$d_s = h_s - z_s \tag{2.3.1}$$

$$m_{sF} = \frac{m_s b_s}{l} \tag{2.3.2}$$

$$m_{sF} = \frac{m_s a_s}{l} \tag{2.3.3}$$

$$\lambda = \frac{k_F}{k_F + k_R} \tag{2.3.4}$$

$$X = \frac{\Delta F_{zF}}{\Delta F_z} \tag{2.3.5}$$

$$X_0 = \lambda \frac{d_s}{h_G}\frac{m_s}{m} + \frac{z_F}{h_G}\frac{m_{sF}}{m} + \frac{h_{uF}}{h_G}\frac{m_{uF}}{m} \tag{2.3.6}$$

$$d_{sF} = h_{sF} - z_F \tag{2.3.7}$$

$$d_{sR} = h_{sR} - z_R \tag{2.3.8}$$

$$\Delta F_{zF} = \left(\frac{k_F d_{sF} m_{sF}}{k_F + \frac{k_R k_C}{k_R + k_C}} + \frac{\frac{k_F k_C}{k_F + k_C} d_{sR} m_{sR}}{k_R + \frac{k_F k_C}{k_F + k_C}} + z_F m_{sF} + h_{uF} m_{uF}\right)\frac{a_y}{t_F} \tag{2.3.9}$$

$$\Delta F_{zR} = \left(\frac{\frac{k_R k_C}{k_R + k_C} d_{sF} m_{sF}}{k_F + \frac{k_R k_C}{k_R + k_C}} + \frac{k_R d_{sR} m_{sR}}{k_R + \frac{k_F k_C}{k_F + k_C}} + z_R m_{sR} + h_{uR} m_{uR}\right)\frac{a_y}{t_R} \tag{2.3.10}$$

$$X = \frac{\lambda^2 - (\mu + 1)\lambda}{\lambda^2 - \lambda - \mu}\frac{d_{sF}}{h_G}\frac{m_{sF}}{m} - \frac{\mu\lambda}{\lambda^2 - \lambda - \mu}\frac{d_{sR}}{h_G}\frac{m_{sR}}{m} + \frac{z_F}{h_G}\frac{m_{sF}}{m} + \frac{z_{uF}}{h_G}\frac{m_{uF}}{m} \tag{2.3.11}$$

Figure 2.2: Jounce (J_i) Evaluation

2.3.2 6-DOF Force Based Roll Center Model

Symbol	Unit	Type	Description
$x, \dot{x}, \ddot{x}$	$m, \frac{m}{s}, \frac{m}{s^2}$	Output	Longitudinal States
$y, \dot{y}, \ddot{y}$	$m, \frac{m}{s}, \frac{m}{s^2}$	Output	Lateral States
$z, \dot{z}, \ddot{z}$	$m, \frac{m}{s}, \frac{m}{s^2}$	Output	Vertical Ride States
$\phi, \dot{\phi}, \ddot{\phi}$	$rad, \frac{rad}{s}, \frac{rad}{s^2}$	Output	Body Roll States
$\theta, \dot{\theta}, \ddot{\theta}$	$rad, \frac{rad}{s}, \frac{rad}{s^2}$	Output	Body Pitch States
$\psi, \dot{\psi}, \ddot{\psi}$	$rad, \frac{rad}{s}, \frac{rad}{s^2}$	Output	Yaw States
$z_{u,i}, \dot{z}_{u,i}, \ddot{z}_{u,i}$	$m, \frac{m}{s}, \frac{m}{s^2}$	Output	Vertical Unsprung States
m_s	kg	Parameter	Sprung Mass
$m_{u,(f\|r)}$	kg	Parameter	Front & Rear Unsprung Mass
I_s	$kg - m^2$	Parameter	Sprung Inertia Tensor
$I_{zz,u}$	$kg - m^2$	Parameter	Unsprung Yaw Inertia
h_s	m	Parameter	Sprung Static CoG Height
$h_{u,(f\|r)}$	m	Parameter	Unsprung Static CoG Height
L	m	Parameter	Wheelbase
$\%_f$	[ ]	Parameter	Front Weight Distribution
$t_{w,i}$	m	Input	Track Width
$k_{r,i}$	$\frac{N}{m}$	Input	Ride Stiffness
$b_{r,i}$	$\frac{N-s}{m}$	Input	Ride Dampening
$\eta_{(f\|s),i}$	deg	Input	Front & Side View Jacking Angle
$d_{(f\|s),i}$	m	Input	Front & Side View Suspension Arm
δ_i	deg	Input	Steer Angle
ω_i	$\frac{rad}{s}$	Input	Rotational Speed
${}_TF_{x,i}$	N	Input	Tire Longitudinal Forces
${}_TF_{y,i}$	N	Input	Tire Lateral Forces
${}_TF_{z,i}$	N	Input	Tire Normal Loads
${}_TM_{z,i}$	N	Input	Tire Aligning Moments
${}_TM_{x,i}$	N	Input	Tire Overturning Moments
${}_AF_x$	N	Input	Aerodynamic Drag Force
${}_AF_y$	N	Input	Aerodynamic Side Force
${}_AF_z$	N	Input	Aerodynamic Downforce
${}_AM_x$	$N - m$	Input	Aerodynamic Roll Moment
${}_AM_y$	$N - m$	Input	Aerodynamic Pitch Moment
${}_AM_z$	$N - m$	Input	Aerodynamic Yaw Moment

Table 2.6: Force Based Roll Center Model Nomenclature

$$\vec{x} = \begin{bmatrix} x \\ y \\ z \end{bmatrix} \qquad \vec{\omega} = \begin{bmatrix} \phi \\ \theta \\ \psi \end{bmatrix} \qquad I_s = \begin{bmatrix} I_{xx,s} & 0 & -I_{xz,s} \\ 0 & I_{yy,s} & 0 \\ -I_{zx,s} & 0 & I_{zz,s} \end{bmatrix}$$

$$m_s \left(\ddot{\vec{x}} + \dot{\vec{\omega}} \times \dot{\vec{x}} \right) + (m_{uf} + m_{ur}) \left(\begin{bmatrix} \ddot{x} \\ \ddot{y} \\ 0 \end{bmatrix} + \begin{bmatrix} 0 \\ 0 \\ \dot{\psi} \end{bmatrix} \times \begin{bmatrix} \dot{x} \\ \dot{y} \\ 0 \end{bmatrix} \right) = \begin{bmatrix} \sum F_{\hat{x}} \\ \sum F_{\hat{y}} \\ \sum F_{\hat{z}} \end{bmatrix} \tag{2.3.12}$$

$$I_s \ddot{\vec{\omega}} + \dot{\vec{\omega}} \times I_s \dot{\vec{\omega}} + \begin{bmatrix} 0 \\ 0 \\ I_{\hat{z}\hat{z},s} \ddot{\psi} \end{bmatrix} = \begin{bmatrix} \sum M_{\hat{x}} \\ \sum M_{\hat{y}} \\ \sum M_{\hat{z}} \end{bmatrix} \tag{2.3.13}$$

$$m_{u,i} \ddot{z}_{u,i} = k_{t,i} \left(z_{r,i} - z_{u,i} \right) - k_{r,i} \left(z_{u,i} - z_{c,i} \right) - b_{r,i} \left(\dot{z}_{u,i} - \dot{z}_{c,i} \right) \tag{2.3.14}$$

Figure 2.3: Rigid Body Equations of Motion for Sprung & Unsprung Masses (6+4-DOF)

$$\sum F_x = \sum_{i=1}^{4} \Big[{}_T F_{x,i} \cos(\delta_i) - {}_T F_{y,i} \sin(\delta_i) \Big] - {}_A F_x \tag{2.3.15}$$

$$\sum F_y = \sum_{i=1}^{4} \Big[{}_T F_{x,i} \sin(\delta_i) + {}_T F_{y,i} \cos(\delta_i) \Big] - {}_A F_y \tag{2.3.16}$$

$$\begin{aligned} \sum F_z = \sum_{i=1}^{4} \Big[& k_{r,i} \mathrm{J}_i + b_{r,i} \dot{\mathrm{J}}_i + \big({}_T F_{x,i} \cos(\delta_i) - {}_T F_{y,i} \sin(\delta_i) \big) \tan(\eta_{s,i}) \\ & + \big({}_T F_{x,i} \sin(\delta_i) + {}_T F_{y,i} \cos(\delta_i) \big) \tan(\eta_{f,i}) \Big] - {}_A F_z \end{aligned} \tag{2.3.17}$$

$$\begin{aligned} \sum M_x = \sum_{i=1}^{4} \Big[& \big({}_T F_{x,i} \sin(\delta_i) + {}_T F_{y,i} \cos(\delta_i) \big) \cdot d_{f,i} \\ & - \big({}_T F_{x,i} \cos(\delta_i) - {}_T F_{y,i} \sin(\delta_i) \big) \tan(\eta_{s,i}) \cdot \frac{t_{w,i}}{2} \Big] \\ & - {}_A F_y \cdot (h_s + z) - {}_A M_x - (k_{\phi f} + k_{\phi r}) \phi - (b_{\phi f} + b_{\phi r}) \dot{\phi} \end{aligned} \tag{2.3.18}$$

$$\begin{aligned} \sum M_y = \sum_{i=1}^{4} \Big[& - \big({}_T F_{x,i} \cos(\delta_i) - {}_T F_{y,i} \sin(\delta_i) \big) \cdot d_{s,i} \\ & + \big({}_T F_{x,i} \sin(\delta_i) + {}_T F_{y,i} \cos(\delta_i) \big) \tan(\eta_{f,i}) \cdot (a \mid b) \Big] \\ & + {}_A F_x \cdot (h_s + z) + {}_A F_z \left(a - \frac{L}{2} \right) - {}_A M_y - k_\theta \theta - b_\theta \dot{\theta} \end{aligned} \tag{2.3.19}$$

$$\begin{aligned} \sum M_z = \sum_{i=1}^{4} \Big[& \big({}_T F_{x,i} \cos(\delta_i) - {}_T F_{y,i} \sin(\delta_i) \big) \cdot \pm \frac{t_{w,i}}{2} \\ & + \big({}_T F_{x,i} \sin(\delta_i) + {}_T F_{y,i} \cos(\delta_i) \big) \cdot (a \mid -b) + {}_T M_{z,i} \Big] \\ & - {}_A F_y \left(\frac{L}{2} - a \right) - {}_A M_z \end{aligned} \tag{2.3.20}$$

Figure 2.4: Force & Moment Evaluation

$$\begin{bmatrix} 1 & 0 & 0 \\ 0 & \cos(\phi) & \sin(\phi) \\ 0 & -\sin(\phi) & \cos(\phi) \end{bmatrix} \begin{bmatrix} \cos(\theta) & 0 & \sin(\theta) \\ 0 & 1 & 0 \\ -\sin(\theta) & 0 & \cos(\theta) \end{bmatrix} \begin{bmatrix} 0 \\ 0 \\ 1 \end{bmatrix} \cdot \begin{bmatrix} (a \mid -b) \\ \mp \frac{t_{(f|r)}}{2} \\ \mathrm{J}_i + z \end{bmatrix} = 0 \tag{2.3.21}$$

$$\mathrm{J}_{w,i} = \mathrm{J}_i - \mathrm{J}_{t,i} \tag{2.3.22}$$

$$\mathrm{J}_{s,i} = \mathrm{J}_{w,i} \cdot R_{s(f|r)} \left(\mathrm{J}_{w,i} \right) \tag{2.3.23}$$

Figure 2.5: Jounce (J_i) Evaluation

$$F_{z,1} = F_{z_0,1} - \frac{K_{\phi f}}{t_f}\phi - F_{y,1}\tan(\eta_{f,1}) - \frac{m_{uf}h_{uf}}{t_f}a_y + \frac{K_\theta}{l}\theta - F_{x,1}\tan(\eta_{s,1}) - \frac{\bar{m}_u\bar{h}_u}{l}a_x \tag{2.3.24}$$

$$F_{z,2} = F_{z_0,2} + \frac{K_{\phi f}}{t_f}\phi + F_{y,2}\tan(\eta_{f,2}) + \frac{m_{uf}h_{uf}}{t_f}a_y + \frac{K_\theta}{l}\theta - F_{x,2}\tan(\eta_{s,2}) - \frac{\bar{m}_u\bar{h}_u}{l}a_x \tag{2.3.25}$$

$$F_{z,3} = F_{z_0,3} - \frac{K_{\phi r}}{t_r}\phi - F_{y,3}\tan(\eta_{f,3}) - \frac{m_{ur}h_{ur}}{t_r}a_y - \frac{K_\theta}{l}\theta + F_{x,3}\tan(\eta_{s,3}) + \frac{\bar{m}_u\bar{h}_u}{l}a_x \tag{2.3.26}$$

$$F_{z,4} = F_{z_0,4} + \frac{K_{\phi r}}{t_r}\phi + F_{y,4}\tan(\eta_{f,4}) + \frac{m_{ur}h_{ur}}{t_r}a_y - \frac{K_\theta}{l}\theta + F_{x,4}\tan(\eta_{s,4}) + \frac{\bar{m}_u\bar{h}_u}{l}a_x \tag{2.3.27}$$

Figure 2.6: Weight Transfer Evaluation, Note: Missing Steer Jacking

$$K_{w(f|r)} = \frac{K_{r(f|r)}K_{t(f|r)}}{K_{t,(f|r)} - K_{r(f|r)}} = K_{s(f|r)} \cdot R^2_{s(f|r)}(\mathrm{J}_{w,i}) \tag{2.3.28}$$

$$K_{\phi_b(f|r)} = K_{\theta_b(f|r)} \cdot R^2_{b(f|r)} \left(\frac{t^2_{(f|r)}}{l^2_{b(f|r)}} \right) \tag{2.3.29}$$

$$K_{\phi(f|r)} = K_{t(f|r)} \left(\frac{t^2_{(f|r)}}{2} \right) \frac{K_{\phi_b(f|r)} + K_{w(f|r)} \left(\frac{t^2_{(f|r)}}{2} \right)}{\left(K_{t(f|r)} + K_{w(f|r)} \right) \left(\frac{t^2_{(f|r)}}{2} \right) + K_{\phi_b(f|r)}} \tag{2.3.30}$$

$$K_\theta = 2a^2K_{rf} + 2b^2K_{rr} \tag{2.3.31}$$

Figure 2.7: Suspension Stiffness Relations - Target Generation, Given: $K_{r(f|r)}$ & $K_{\phi(f|r)}$

2.4 Chassis Model Management

Chapter 3

Wheel & Tire Dynamics

3.1 Rotational Dynamics

The most basic degree of freedom at the wheel package is the axial rotation about the nominal y-axis. This degree of freedom is essential to longitudinal performance of the tire as the calculation of slip ratio is dependent on the angular rate of the wheel and tire.

This model simplifies the dynamics of the rotating wheel to a profile view. The diagram below does not depict the additional moment contributed by the normal force to avoid cluttering the diagram.

Symbol	Unit	Type	Description
$F_{x,i}$	N	Input	Longitudinal Force
$F_{B,i}$	N	Input	Braking Force
$\tau_{D,i}$	Nm	Input	Drive Torque
ω_i	$\frac{rad}{s}$	Output	Rotational Rate of Wheel
r_e	m	Variable	Effective Radius of the Tire
r_r	m	Parameter	Rotor Radius
J_i	kgm^2	Parameter	Inertia of Axle Assembly
b_i	Nms	Parameter	Dampening of Axle Assembly

Table 3.1: Planar Wheel Model Nomenclature

Note that the moment contributed by the normal load can typically be ignored as they don't contribute much to the dynamics and the rolling resistance of the tire is much more imperative. Yet, without in-house empirical testing it is impossible to accurately describe this as the FSAE Tire Testing Consortium (TTC) isn't capable of providing that data. The rotor radius has been historically synonymous across all four corners, while the inertia and dampening is consistent for each axle but differs front to rear due to tripods and half shafts. The effective radius for higher fidelity is a function of normal load on each tire; however, for lower fidelity sweeps it may be assumed a constant.

$$\dot{\omega}_i J_i + \omega_i b_i = \tau_{D,i} - F_{x,i} r_e - F_{b,i} r_r \tag{3.1.1}$$

It is also note worthy that the longitudinal and vertical forces are not balanced here and those are balanced in other systems that are typically accounted for by chassis dynamics models.

Sources: N/A

Contributor	Date	Changes
Blake Christierson	3/24/20	First Draft

3.2 Tire Slip Estimation

3.2.1 Slip Angle

3.2.2 Slip Ratio

3.3 Linear Cornering Coefficients

3.4 Pacejka Magic Formula 6.2 (MF6.2)

3.4.1 Pure Slip Fitting

Longitudinal Force

Lateral Force

Aligning Moment

3.4.2 Combined Slip Fitting

Steady State Forces

Aligning Moment

Overturning Moment

3.4.3 Modifications & Extensions

Thermal Models

3.5 Nicolas-Comstock-Brach Combined Slip Model

3.6 Transient Dynamics

3.6.1 Relaxation Length Models

Lateral Force

In addition to steady-state force response, the tire also exhibits a time-dependent transient force response. This is the delay in the buildup of the cornering force in the lateral direction, which is often characterized by the tire relaxation length. Thus, the shorter the relaxation length, the faster the buildup of the cornering force in the lateral direction, and the more responsive the vehicle handling performance since relaxation length is one of the factors.

The lateral force relaxation length model obtains the values of relaxation length as a function of tire inflation pressure and normal load for different tires to allow comparison between the tire's contribution to the vehicle handling performance during transient-state.

This model uses raw transient tests tire data from the FSAE Tire Testing Consortium (TTC) which are segmented to provide individual instances of the buildup of the cornering force. The segmentation is achieved by first identifying a reference variable to cornering force, which in this case is the belt velocity. This conclusion is made after comparing the cornering force plot against time with other available tire variables, and it was discovered that the belt velocity plot against time indicate the individual cornering force buildup the best because the instant the belt velocity increases to steady-state from rest is the instant at which the buildup of the cornering force occurs.

After the first data segmentation, the following two steps are done chronologically to segment the raw data into 27 distinct data since there are three different inflation pressure, normal load, and slip angle applied:

1. Filtering out the data when tire is not rolling.
2. Filtering out the data when steady-state velocity data points exceed its average because it is where the cornering force buildup occurs.

Using the segmented data and Equation 3.6.1, curve fitting is done to obtain the values of tau, τ, which will be used to calculate the relaxation length represented in λ for each case.

$$\dot{F}_y = F_{y_{t\to\infty}}\left[1 - \exp\left(-\frac{t}{\tau}\right)\right] \tag{3.6.1}$$

$$\tau = \frac{K_{y\alpha}}{\dot{x}_t k_{yy}} \tag{3.6.2}$$

$$\lambda = \tau \dot{x}_t \tag{3.6.3}$$

These calculated relaxation lengths will then be categorized per slip angle applied and averaged for comparison between different tires. The tire with the shorter average relaxation lengths is preferred because it would contribute in having a more responsive vehicle.

Note: The curve fitting done to obtain the relaxation length values is first-order. This is because it is accurate enough to project the tire's contribution to vehicle handling performance in transient-state at the moment the lateral force relaxation length model is first completed such that the second-order curve fitting is left for when more accurate data is required to justify tire choice.

Aligning Moment

3.7 Tire Model Management

Chapter 4

Aerodynamics

4.1 Aerodynamic Slip

4.2 Aerodynamic Model Management

Chapter 5

Suspension Dynamics

5.1 Simple Weight Transfer

$$\begin{aligned}
\sum F_y: &\quad ma_y = F_{y,1} + F_{y,2} \\
\sum F_z: &\quad 0 = F_{z,1} + F_{z,2} - mg \\
\sum M_x: &\quad 0 = (F_{y,1} + F_{y,2}) \cdot h + F_{z,1} \cdot \frac{1}{2} t_w - F_{z,2} \cdot \frac{1}{2} t_w
\end{aligned}$$

$$\begin{aligned}
\sum F_y: &\quad ma_y = 0 \\
\sum F_z: &\quad 0 = F_{z,1} + F_{z,2} - mg \\
\sum M_x: &\quad 0 = F_{z,1} \cdot \frac{1}{2} t_w - F_{z,2} \cdot \frac{1}{2} t_w
\end{aligned}$$

$$\begin{aligned}
\text{From } \sum M_x: &\quad F_{z,1} = F_{z,2} \\
\text{Subbing into } \sum F_z: &\quad F_{z,1} = F_{z,2} = \frac{1}{2} mg
\end{aligned}$$

$$\begin{aligned}
\sum F_y: &\quad ma_y = F_y \\
\sum F_z: &\quad 0 = F_{z,1} + F_{z,2} - mg \\
\sum M_x: &\quad 0 = F_y \cdot h + F_{z,1} \cdot \frac{1}{2} t_w - F_{z,2} \cdot \frac{1}{2} t_w
\end{aligned}$$

$$\begin{aligned}
\text{From } \sum M_x: &\quad F_{z,2} = F_{z,1} + F_y \frac{2h}{t_w} \\
\text{Subbing into } \sum F_z: &\quad \begin{aligned} F_{z,1} &= \tfrac{1}{2} mg - F_y \tfrac{h}{t_w} \\ F_{z,2} &= \tfrac{1}{2} mg + F_y \tfrac{h}{t_w} \end{aligned}
\end{aligned}$$

5.2 Low Fidelity Kinematic Response Surface Forms

$$\delta = \delta_0 + k_{\delta_r}\delta_r + k_{\delta_{r^2}}\delta_r^2 + k_{\delta_{r^3}}\delta_r^3 + k_{\delta_{\mathrm{j}}\mathrm{J}} + k_{\delta_{r\mathrm{j}}}\delta_{r\mathrm{J}} \tag{5.2.1}$$

$$\gamma(\delta, \mathrm{j}) = \gamma_0 + \left[-\varphi\delta + \frac{1}{2}\Gamma\,\mathrm{sgn}(\delta)\delta^2\right] - \int_0^{\mathrm{J}} \arctan\left(\frac{1}{FVSA(\mathrm{j})}\right) d_{\mathrm{J}} \tag{5.2.2}$$

$$FVSA = \left\|\vec{CP}(\mathrm{j}) - \vec{IC}(\mathrm{j})\right\|_2 \tag{5.2.3}$$

5.3 Jounce Conventions & Vertical Nonlinearities

The vertical modes of the sprung and unsprung masses are largely affected by the nonlinear nature of the kinematic and compliances present in suspending the car. The ultimate consequence of these considerations is the deducing of the correct length of the push rod so that ride height targets are met for given spring rate targets and static load distribution. The formulation will also allow for tire lift and determining whether bump stops are met in the shock.

Jounce is defined as an upward motion of the unsprung mass relative to the sprung mass. The definition of the origin of jounce is difficult and is ambiguous if it should be at static ride conditions or at full droop. To remove the dependency of the origin on spring choice and solely place the origin's dependence on kinematics the origin, j = 0, is defined as the full droop position (fully extended shock with even tires if a decoupled shock setup).

The first nonlinearity to discuss is the shock spring which produces a spring force (F_s) as a function of spring displacement (δ_s). The considerations here are spring rate (k_s), preload ($\delta_{s,p}$), spring rate nonlinearity ($k_n \approx 0.01\%$ of k_s), and piecewise nature of bump stops ($k_b \approx 1000k_s$), and the physical free length (l) and stroke (s) of the chosen shock. The spring rate nonlinearity for linear springs is largely negligible; however, progressive springs will have significant nonlinearities and are of potential interest to tune weight transfer at varying operating conditions.

$$F_s(\delta_s) = \begin{cases} k_s(s + \delta_{s,p}) + k_n(s + \delta_{s,p})^3 + k_b(l - s - \delta_s) & \text{if } \delta_s < l - s \\ k_s(l - \delta_s + \delta_{s,p}) + k_n(l - \delta_s + \delta_{s,p})^3 & \text{if } l - s \leq \delta_s < l \\ k_s\delta_{s,p} + k_n\delta_{s,p}^3 + k_b(l - \delta_s) & \text{if } l \leq \delta_s \end{cases} \tag{5.3.1}$$

The tire spring is also highly nonlinear and very similar to the shock spring without bump stop stiffnesses. The other important difference is that the tire cannot provide tensile forces:

$$F_{z,t}(r) = \begin{cases} k_t(r_0 - r) + k_n(r_0 - r)^3 & \text{if } r \leq r_0 \\ 0 & \text{if } r > r_0 \end{cases} \tag{5.3.2}$$

5.4 Simplified Kinematics Multibody System

Symbol	Frame	Description
I	Intermediate	Ground aligned system beneath c.g.
B	Body	Sprung mass frame at sprung mass c.g.
$(F\|R)(L\|U)A$	A-Arm	Double wishbone suspension member aligned with body
$(F\|R)TR$	Tie Rod	
$(F\|R)R$	Rocker	
$(F\|R)S$	Shock	
$(F\|R)PR$	Pushrod	

Table 5.1: Kinematics model coordinate systems

5.4.1 Roll & Steer Geometry Development

The body frame is centered about the sprung mass center of gravity (cg) and is related to the intermediate coordinate system via pitch and roll. Note that by working in the intermediate frame the global position (X,Y,0) and yaw heading is not relevant:

$$ {}^{B}O^{I} = (0, 0, z_{cg}) \qquad {}^{B}R^{W} = {}^{B}R^{I}(\phi, \theta, 0) \tag{5.4.1} $$

All inboard pickups are defined in the body frame. This includes: A-arms, tie rods, rockers, and shocks as well as anti-roll bars or heave springs. Below is how we define the A-arm coordinate systems, note that α_1, α_2 are design constants defining the rotation axis of the inboard revolute joint which effects anti-dive and anti-squat as well as swing arm geometry, while β is the dynamic rotation angle state related to the A-arm pivoting on the revolute joint. The revolute joint arises from the two inboard hard points fixed to the body frame, meanwhile the third hard point is the apex which is free to move about the rotational DoF. One A-arm in each axle also has an outboard pickup point for vertical forces (PRB) which the push or pull rod connects to. The Δ_φ is a longitudinal perturbation in the apex due to caster and is solved for during the design generation.

$$ \begin{aligned} {}^{(L|U)A}O^{B} &= p^{B}_{(L|U)A} = (\pm L/2 \pm \Delta_\varphi, y_{(L|U)A}, z_{(L|U)A}) \\ {}^{(L|U)A}R^{B} &= {}^{(L|U)A}R^{B}_{x}(\beta)\, {}^{(L|U)A}R^{B}(0, \alpha_1, \alpha_2) \end{aligned} \tag{5.4.2} $$

The tie rod frame is defined with fixed lateral rotation due to that specific degree of freedom being unconstrained:

$$ {}^{TR}O^{B} = p^{B}_{TA} \qquad {}^{TR}R^{B} = {}^{TR}R^{B}(\beta_1, 0, \beta_2) \tag{5.4.3} $$

Next, the tire coordinate system is defined on the ground at the approximate center of the contact patch with both steer and camber angle accounted for. The wheel coordinate system is then defined by a vertical displacement of the loaded radius in the intermediate frame and then caster is applied.

$$ {}^{T}O^{I} = (L/2, t_{w,(F|R)}/2, 0) \qquad {}^{T}R^{I} = {}^{T}R^{W}(\gamma, 0, \delta) \tag{5.4.4} $$

$$ {}^{W}O^{T} = (0, 0, r_l/\sin(\pi/2 - \gamma)) \qquad {}^{W}R^{T} = {}^{T}R^{W}(0, \varphi, 0) \tag{5.4.5} $$

For solution purposes, we define a lower ball joint coordinate system relative to the lower A-Arm frame and Tire frame. This allows for the vector loop to be written effectively:

$$^{LB}O^{LA} = (0, L_{LA}, 0) \qquad ^{LB}R^{LA} = {}^{LB}R^{LA}(\beta_1, \beta_2, \beta_3) \tag{5.4.6}$$

$$^{LB}O^{T} = (0, -Y^T_{LB}, -Z^T_{LB}) \qquad ^{LB}R^{T} = {}^{LB}R^{T}(0, 0, 0) \tag{5.4.7}$$

The tire frame holds relationships for the upper ball joint (UB), lower ball joint (LB), and Tie Rod Pickup (TB).

$$p^T_{UB} : (0, Y^T_{UB}, Z^T_{UB}) = p^{UA}_{UB} : (0, L_{UA}, 0) = p^{LB}_{UB} : (0, Y^T_{UB} - Y^T_{LB}, Z^T_{UB} - Z^T_{LB}) \tag{5.4.8}$$

$$p^T_{LB} : (0, Y^T_{LB}, Z^T_{LB}) = p^{LA}_{LB} : (0, L_{LA}, 0) = p^{LB}_{LB} : (0, 0, 0) \tag{5.4.9}$$

$$p^T_{TB} : (X^T_{TB}, Y^T_{TB}, Z^T_{TB}) = p^{TR}_{TB} : (0, L_{TR}, 0) = p^{LB}_{TB} : (X^T_{TB}, Y^T_{TB} - Y^T_{LB}, Z^T_{TB} - Z^T_{LB}) \tag{5.4.10}$$

The first vector loop for the consistency of the Upper Ball Joint (UB) may be written as:

$$p^{UA}_{UB} = p^{LB}_{UB} \tag{5.4.11}$$

$$^{B}T^{UA}\left(p^{UA}_{UB}\right) = {}^{B}T^{LA}\left({}^{LA}T^{LB}\left(p^{LB}_{UB}\right)\right) \tag{5.4.12}$$

The second vector loop for the consistency of the Outboard Tie Rod Joint (TB) may be written as:

$$(p_{TB} - p_{TA})^{TR} = (p_{LA} - p_{TA})^{B} + (p_{LB} - p_{LA})^{LA} + (p_{TB} - p_{LB})^{LB} \tag{5.4.13}$$

$$p^{TR}_{TB} = (p_{LA} - p_{TA})^{B} + p^{LA}_{LB} + p^{LB}_{TB} \tag{5.4.14}$$

$$^{B}T^{TR}\left(p^{TR}_{TB}\right) = (p_{LA} - p_{TA})^{B} + {}^{B}T^{LA}\left(p^{LA}_{LB}\right) + {}^{B}T^{LA}\left({}^{LA}T^{LB}\left(p^{LB}_{TB}\right)\right) \tag{5.4.15}$$

The third vector loop for the consistency of the Wheel Hub ($^{W}O^{T}$) in the world and lower ball joint plane may be written as:

$$^{W}O^{T} = (p_{LB} - p_{LA})^{LA} + (p_{T} - p_{LB})^{LB} \tag{5.4.16}$$

$$^{W}O^{T} = p^{LA}_{LB} + p^{LB}_{T} \tag{5.4.17}$$

$$^{W}O^{T} = {}^{W}T^{B}\left({}^{B}T^{LA}\left(p^{LA}_{LB}\right)\right) + {}^{W}T^{B}\left({}^{B}T^{LA}\left({}^{LA}T^{LB}\left(p^{LB}_{T}\right)\right)\right) \tag{5.4.18}$$

The are 8 unknown parameters in the transformations in the vector loop kinematic equations. These eight transformation angles are solved for using the MATLAB optimization solver, fmincon():

$$^{B}T^{LA} \;:\; {}^{B}\beta^{LA} \tag{5.4.19}$$

$$^{B}T^{UA} \;:\; {}^{B}\beta^{UA} \tag{5.4.20}$$

$$^{B}T^{TR} \;:\; {}^{B}\beta^{TR}_{1}, {}^{B}\beta^{TR}_{2} \tag{5.4.21}$$

$$^{LA}T^{LB} \;:\; {}^{LA}\beta^{LB}_{1}, {}^{LA}\beta^{LB}_{2}, {}^{LA}\beta^{LB}_{3} \tag{5.4.22}$$

$$^{W}T^{T} \;:\; \frac{t_w}{2}, (a|b) \tag{5.4.23}$$

Wheel package kinematic goals are more commonly discussed in terms of kingpin inclination (KPI, Γ), mechanical scrub (s_m), and mechanical trail (t_m) in conjunction with

tire orientation.

$$\Gamma = \arctan\left(\frac{Y^T_{(F|R)UB} - Y^T_{(F|R)LB}}{Z^T_{(F|R)UB} - Z^T_{(F|R)LB}}\right) \tag{5.4.24}$$

$$s_m = \frac{Y^T_{(F|R)UB} - Y^T_{(F|R)LB}}{Z^T_{(F|R)UB} - Z^T_{(F|R)LB}}\left(-r_e - Z^T_{(F|R)LB}\right) + Y^T_{(F|R)LB} \tag{5.4.25}$$

$$t_m = r_e \tan(\varphi) \tag{5.4.26}$$

The tie rod is also determined in the wheel package. Unlike most other components, its outboard pickup is set first and its inboard pickup is chosen for bump steer and Ackerman objectives.

1. Provide Static Targets:
   - Wheelbase: L
   - Nominal Track Width: t_w
   - Static Ride Height: z_0
   - Rake Angle: θ_0
   - Tire Effective Radius: r_e
   - Force-Based Roll Center: c_{RC}
   - Caster: φ
   - Static Camber: γ_0
   - Kingpin Inclination or Mechanical Scrub: $\Gamma|s_m$
   - Camber Gain: $\frac{d\gamma}{d\mathfrak{j}}$
   - Static Toe: δ_0
2. Provide Bounds for Design Variables:
   - A-Arm Inboard Pickups: $(Y^B_{(F|R)(L|U)A}, Z^B_{(F|R)(L|U)A})$
   - A-Arm Upright Pickups: $(Y^T_{(L|U)BJ}, Z^T_{(L|U)BJ})$
   - Tie Rod Inboard Pickups: $(X^B_{TRB}, Y^B_{TRB}, Z^B_{TRB})$
   - Tie Rod Upright Pickups: $(X^T_{TRT}, Y^T_{TRT}, Z^T_{TRT})$
3. Solve for Following from KPI, Roll Center, and Camber Objectives
   - Bounded Design Variables
   - Tie Rod Length
   - A-Arm Length
4. Sweep Rack Displacement and Body Attitude (Robust Performance)

Objectives in Order of Importance

- Maximize Tire Performance
  - Optimize Slip Angle
  - Optimize Camber
- Minimize Compliance
  - Maximize Toe Base
  - Maximize Ball Joint Arms
- Manage Driver Effort
  - Maximize Toe Base
  - Optimize Caster

5.4.2 MATLAB Kinematics Optimization

This section focuses on the documentation and explanation of the Current MATLAB Kinematics Model.

First we begin with Target and Bound initialization:

Name	Value	Description	Units
$Target.Wheelbase$	1525	Wheelbase Length	mm
$Target.WeightDist$	0.5	Weight Distribution	%
$Target.SprungMass$	225	Sprung Mass Weight	kg

Table 5.2: Kinematics model Nomenclature

$$FVSA = \frac{1}{tan(|Camber\ Gain|)} \tag{5.4.27}$$

$$WheelCirc = -\sqrt{FVSA^2 - (z - Target.Rl^2)} + \frac{Target.Track}{2} \tag{5.4.28}$$

$$ForceLine = (z - Target.RollCenter) * \frac{-T_w}{2 * Target.RollCenter} \tag{5.4.29}$$

$$\tag{5.4.30}$$

5.4.3 Pushrod & Pullrod Kinematics Development

$$^BO^R = p^B_{RA} \qquad ^BR^R = {}^BR^R_x(\beta)\ {}^BR^R(0, \alpha_1, \alpha_2) \tag{5.4.31}$$

Talk about solving for $\alpha_{1,2}$ by aligning the x-axis of the rocker frame to the normal of the plane defined by p^B_{SA}, p^B_{RA}, and $p^{(L|U)A}_{PB}$ all at the ride height condition $z = z_r$.

There are two important points in the rocker frame:

$$p^R_{PA} = (0, L_{R,1}, 0) \tag{5.4.32}$$

$$p^R_{SB} = (L_{R,2}\cos\theta_R, L_{R,2}\sin\theta_R, 0) \tag{5.4.33}$$

Need to find ride height spring compression to compute the length of the pushrod. This is nonlinear and needs to be iterated to solve for the proper compression and pushrod length. After this, the spring length can just be a measurement. This gives L_{PR} and β_0 of ${}^BR^R$. Suggest initial guess for spring displacement is 3/4 of the total shock displacement.

1. Compute Static Rocker Plane & Normal Vector

5.5 Suspension Linkage Forces

Symbol	Unit	Type	Description
F_y	N	Output	Lateral Force
F_z	N	Input	Normal Force
F_x	N	Output	Longitudinal Force

Table 5.3: Six-Link Model Nomenclature

$$F_y = 0 \tag{5.5.1}$$

$$F_x = \frac{\frac{\mu W b}{L}}{1 - \frac{h}{L}\mu} \tag{5.5.2}$$

$$F_z = W * (\frac{c}{L} - \frac{a_x}{g}\frac{h}{L}) \tag{5.5.3}$$

Braking Performance

$$D_x = \frac{F_{xmf} + F_{xr}}{W} \tag{5.5.4}$$

$$F_{xmf} = \frac{\mu_p(W_{fs} + \frac{h}{L}F_{xr})}{1 - \mu_p\frac{h}{L}} \tag{5.5.5}$$

$$F_b = G\frac{P_a}{r} \tag{5.5.6}$$

$$F_y = 0 \tag{5.5.7}$$

$$F_x = \mu_p * (W_{fs} + \frac{W D_x h}{L}) \tag{5.5.8}$$

$$F_z = W_{fs} + \frac{W D_x h}{L} \tag{5.5.9}$$

Chapter 6

Controls Systems Dynamics

6.1 Inboard Steering

6.1.1 Simple Gains Steering Model

6.1.2 Compliant Inboard Steering Bond Graph Model

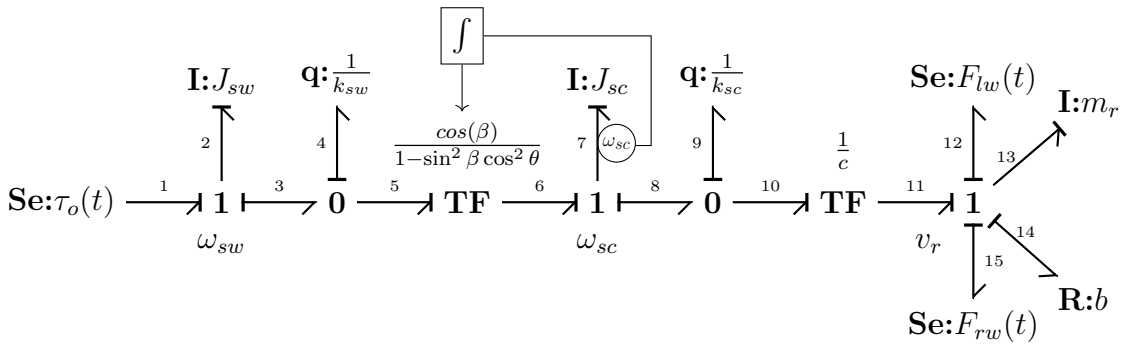

Figure 6.1: Compliant Inboard Steering Bond Graph

$$
\begin{aligned}
\dot{H}_{sw} &= e_2 \\
&= e_1 - e_3 \\
&= \tau_o(t) - e_4 \\
&= \tau_o(t) - k_{sw}q_{sw}
\end{aligned}
$$

$$
\begin{aligned}
\dot{q}_{sw} &= f_4 \\
&= f_3 - f_5 \\
&= f_2 - f_7(\frac{cos(\beta)}{1-\sin^2\beta\cos^2\theta}) \\
&= \frac{1}{J_{sw}} - f_6(\frac{cos(\beta)}{1-\sin^2\beta\cos^2\theta}) \\
&= \frac{H_{sw}}{J_{sw}} - \frac{H_{sc}}{J_{sc}}(\frac{cos(\beta)}{1-\sin^2\beta\cos^2\theta})
\end{aligned}
$$

$$
\begin{aligned}
\dot{H}_{sc} &= e_7 \\
&= e_6 - e_8 \\
&= e_5(\frac{cos(\beta)}{1-\sin^2\beta\cos^2\theta}) - e_9 \\
&= e_4(\frac{cos(\beta)}{1-\sin^2\beta\cos^2\theta}) - k_{sc}q_{sc} \\
&= k_{sw}q_{sw}(\frac{cos(\beta)}{1-\sin^2\beta\cos^2\theta}) - k_{sc}q_{sc}
\end{aligned}
$$

$$
\begin{aligned}
\dot{q}_{sc} &= f_9 \\
&= f_8 - f_{10} \\
&= f_7 - f_{11}\frac{1}{c} \\
&= \frac{H_{sc}}{J_{sc}} - f_{13}\frac{1}{c} \\
&= \frac{H_{sc}}{J_{sc}} - \frac{p_r}{m_r}\frac{1}{c}
\end{aligned}
$$

$$
\begin{aligned}
\dot{p}_r &= e_{13} \\
&= e_{11} - e_{12} - e_{14} - e_{15} \\
&= e_{10}\frac{1}{c} - F_{lw}(t) - b(f_{14}) - F_{rw}(t) \\
&= k_{sc}q_{sc}\frac{1}{c} - F_{lw}(t)\frac{b}{m_r}p_r - F_{rw}(t)
\end{aligned}
$$

$$\underline{\dot{\vec{x}} = A\vec{x} + B\vec{u}}:$$

$$\begin{bmatrix} \dot{H}_{sw} \\ \dot{q}_{sw} \end{bmatrix} = \begin{bmatrix} 0 & -k_{sw} \\ \frac{1}{J_{sw}} & 0 \end{bmatrix} \begin{bmatrix} H_{sw} \\ q_{sw} \end{bmatrix} + \begin{bmatrix} 1 & 0 \\ 0 & -1 \end{bmatrix} \begin{bmatrix} \tau_o \\ \omega_{uj} \end{bmatrix}$$

$$\underline{\dot{\vec{y}} = C\vec{x} + D\vec{u}}:$$

$$\begin{bmatrix} \omega_{sw} \\ \tau_{uj} \end{bmatrix} = \begin{bmatrix} \frac{1}{J_{sw}} & 0 \\ 0 & k_{sw} \end{bmatrix} \begin{bmatrix} H_{sw} \\ q_{sw} \end{bmatrix} + \begin{bmatrix} 0 & 0 \\ 0 & 0 \end{bmatrix} \begin{bmatrix} \tau_o \\ \omega_{uj} \end{bmatrix}$$

Figure 6.2: State space model for left side of universal joint transformer

$$\underline{\dot{\vec{x}} = A\vec{x} + B\vec{u}}:$$

$$\begin{bmatrix} \dot{H}_{sc} \\ \dot{q}_{sc} \\ \dot{p}_r \end{bmatrix} = \begin{bmatrix} 0 & -k_{sc} & 0 \\ \frac{1}{J_{sc}} & 0 & \frac{-1}{c(m_r)} \\ 0 & \frac{1}{c}k_{sc} & \frac{-b}{m_r} \end{bmatrix} \begin{bmatrix} H_{sc} \\ q_{sc} \\ p_r \end{bmatrix} + \begin{bmatrix} 1 & 0 & 0 \\ 0 & 0 & 0 \\ 0 & -1 & -1 \end{bmatrix} \begin{bmatrix} \tau_{uj} \\ F_{lw} \\ F_{rw} \end{bmatrix}$$

$$\underline{\dot{\vec{y}} = C\vec{x} + D\vec{u}}:$$

$$\begin{bmatrix} \omega_{uj} \end{bmatrix} = \begin{bmatrix} \frac{1}{J_{sc}} & 0 & 0 \end{bmatrix} \begin{bmatrix} H_{sc} \\ q_{sc} \\ p_r \end{bmatrix} + \begin{bmatrix} 0 & 0 & 0 \end{bmatrix} \begin{bmatrix} \tau_{uj} \\ F_{lw} \\ F_{rw} \end{bmatrix}$$

Figure 6.3: State space model for right side of universal joint transformer

6.2 Braking System

6.2.1 Simple Gains Brake Model

6.2.2 Bond Graph Brake Model

Chapter 7

Powertrain Dynamics

This chapter focuses on the various models used to capture the effects of how power is transmitted to the wheels. As of March 2020, the current architecture of FRUCD cars is a rear wheel drive system powered by a single electric motor whose torque is distributed via a torque sensitive differential. The majority of the developed models and planned work is focused around this architecture. It should be noted, with the inevitability of the change to a hub based all wheel drive system for performance gains, the future models used to design such a system may have to have a slightly different implementation within the vehicle simulator. However, they should be able to work within the larger current framework and arrangement of the subsystems.

7.1 Simple Gains Powertrain Model

7.2 Medium Fidelity Powertrain Model

The powertrain medium fidelity model has two primary purposes of generating accumulator current draw cycles as well as tuning differential behavior to understand how various tunes affect yaw response. The main tuning parameter at this level is the final drive ratio or the gearing ratio between the motor sprocket and axle sprocket. This has trade-offs between max speed and acceleration as well as system efficiency which leads to energy consumption.

The only state equations directly attributed to the powertrain model relates to the dynamics of the differential and motor. The other two state equations are from the wheel speed model. All of the equations come directly from Newton's 2nd Law when applied to a rotational system.

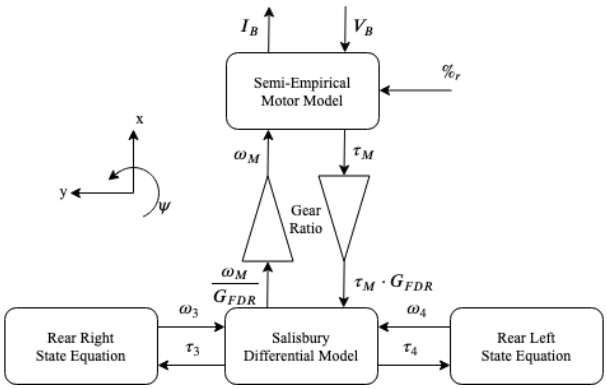

Figure 7.1: Powertrain Medium Fidelity Model Block Diagram

Symbol	Unit	Type	Description
V_B	V	Input	Voltage Supplied to Motor
$\%_r$	[ ]	Input	Torque Request $\in [0, 1]$
I_B	A	Output	Current Drawn by Motor
τ_M	Nm	Variable	Torque Supplied By Motor
ω_M	$\frac{rad}{s}$	Variable	Motor Rotational Speed
τ_A	Nm	Variable	Total Axle Drive Torque
$\tau_{3,4}$	Nm	Variable	Rear Left & Right Drive Torque
$\omega_{3,4}$	$\frac{rad}{s}$	Variable	Rear Left & Right Rotational Speed
G_{FDR}	[ ]	Parameter	Final Drive Ratio (Gearing Ratio)
$J_{M,D}$	kgm^2	Constant	Inertia of Motor or Differential Assembly
$b_{M,D}$	Nms	Constant	Dampening of Motor or Differential Assembly
$\eta_{M,D}$	[ ]	Constant	Motor or Differential Efficiency

Table 7.1: Powertrain Medium Fidelity Model Nomenclature

It is difficult to estimate the differential dampening coefficient and efficiencies as constants for this model. Some empirical testing should be done to more accurately

determine these constants. In the time being, the dampening is chosen such that the response time of the first order equation makes reasonable sense. This does not have a large effect in the transients as back emfs of the motor make much more of an influence. The efficiency is taken as a function of the differential torque and is detailed in the Salisbury model for now. The wheel rotational equations of state are repeated below for ease of reference. More detail about the nomenclature for those equations are available in the dedicated chapter.

$$\dot{\omega}_M J_M + \omega_M b_M = \tau_M - r_M F_C \tag{7.2.1}$$
$$\dot{\omega}_D J_D + \omega_D b_D = \eta_C r_D F_C - \tau_A \tag{7.2.2}$$

$$\dot{\omega}_3 J_3 + \omega_3 b_3 = \eta_D \tau_3 - F_{x,3} r_e - F_{b,3} r_r \quad \text{(Revisited, 3.1.1)}$$
$$\dot{\omega}_4 J_4 + \omega_4 b_4 = \eta_D \tau_4 - F_{x,4} r_e - F_{b,4} r_r \quad \text{(Revisited, 3.1.1)}$$

Note, that by allowing the chain slack and compliance to be negligible to the transient response of the system, the following constraints may be applied and the state equations directly attributable to the system may be resolved into the one below by substituting the constraints into Equation 7.2.2:

$$\tau_D = \tau_M \cdot G_{FDR} \tag{7.2.3}$$
$$\omega_D = \frac{\omega_M}{G_{FDR}} \tag{7.2.4}$$

$$\dot{\omega}_M \left(J_M + \frac{J_D}{G_{FDR}} \right) + \omega_M \left(b_M + \frac{b_D}{G_{FDR}} \right) = \tau_M \left(\eta_M + \eta_D \cdot G_{FDR} \right) - \tau_A \tag{7.2.5}$$

See Section 7.2.3 for how these equations and the constraints applied in the following sections are implemented within the vehicle simulator.

Sources: N/A

Contributor	Date	Changes
Blake Christierson	3/20/20	First Draft

7.2.1 Salisbury Differential Model

The first goal with the differential is to induce locking at the appropriate time on corner exit to provide power to the outside wheel instead of the inside wheel that is unloaded due to weight transfer. This is not possible when the differential is open as is the optimal case during the majority of turning as the wheels will traverse significantly different distances in a tight corner and thus will be turning at different speeds. There is also an effect on corner entry from "engine braking". For amateur drivers, the goal is to induce an understeer moment in braking to keep the car stable in the rear, and then a slight oversteer moment, while still maintaining stability, to allow the driver to power on the throttle earlier in the exit for a higher straight line speed.

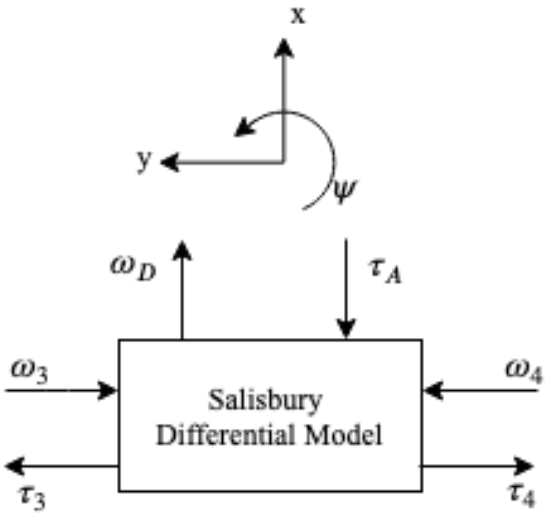

Figure 7.2: Salisbury Model Block Diagram

Symbol	Unit	Type	Description
τ_A	Nm	Input	Total Axle Drive Torque
$\omega_{3,4}$	$\frac{rad}{s}$	Input	Left & Right Wheel Speeds
$\tau_{3,4}$	Nm	Output	Left & Right Drive Torques
ω_D	$\frac{rad}{s}$	Output	Rotational Speed of Differential
η_D	[ ]	Output	Differential Efficiency
$\Delta\tau$	Nm	State	Differential Torque
$\sigma_{D,B}$	deg	Parameter	Drive & Brake Ramp Angles
$\tau_{D,B}$	Nm	Parameter	Drive & Brake Preload Torque
r_{Ramp}	m	Constant	Ramp Radius
r_o	m	Constant	Outer Radius of Clutch Packs
r_i	m	Constant	Inner Radius of Clutch Pack
μ_c	[ ]	Constant	Clutch Coefficient of Friction
N	[ ]	Constant	Number of Friction Surfaces

Table 7.2: Salisbury Model Nomenclature

Most of the constants in this model can be derived easily from the CAD of the differential in question. The major conundrum is estimating the friction coefficient of the clutch pads due to the viscosity of the fluid and how it interacts with the friction material. This would be best estimated in both a dynamic and static friction test with the differential isolated to approximate a non-linear friction model. It should be noted that the preload torque in braking and drive are typically the same, $\tau_D = \tau_B$.

The Salisbury model does not contain any state equations, instead it is comprised of constraint equations applied to the larger powertrain medium fidelity model to relate the inputs and outputs. These constraint equations are different whether the applied torque exceeds the preload torque. If the applied torque exceeds the preload torque then the clutches are allowed to slip and thus begin to distribute differential torque; however, if the applied torque is below that threshold then the friction force cannot be overcome.

$$\begin{cases} \omega_D = \omega_3 = \omega_4, & \text{if } \tau_A \in [\tau_B, \tau_D] \\ \omega_D = \frac{1}{2}\left(\omega_3 + \omega_4\right), & \text{otherwise} \end{cases} \tag{7.2.6}$$

$$\begin{cases} \tau_A = \tau_3 + \tau_4, & \text{if } \tau_A \in [\tau_B, \tau_D] \\ \begin{cases} \tau_3 = \frac{1}{2}\tau_A - \operatorname{sgn}\left(\Delta\omega\right) \cdot \Delta\tau \\ \tau_4 = \frac{1}{2}\tau_A + \operatorname{sgn}\left(\Delta\omega\right) \cdot \Delta\tau \end{cases}, & \text{otherwise} \end{cases} \tag{7.2.7}$$

The following intermediary equations are used to calculate some of the values used in the constraint equations above:

$$\Delta\omega = \omega_3 - \omega_4 \tag{7.2.8}$$

$$\Delta\tau = \left(\frac{\tau_A}{r_{Ramp}} \cdot \cot\left(\sigma_{D,B}\right)\right)\left(\frac{2}{3} \cdot \frac{r_o^3 - r_i^3}{r_o^2 - r_i^2}\right)\left(\mu_c N\right)\left(|\Delta\omega| \cdot \tanh\left(4|\Delta\omega|\right)\right) \tag{7.2.9}$$

While the differential speed is straight forward, the differential torque is somewhat more complicated. It has been as is above in parentheses to help compartmentalize the different aspects of the formula as below.

$$\Delta\tau = F_c \cdot r_{eff} \cdot f_c \cdot \mathrm{f}(|\Delta\omega|)$$

Where the first segment is the normal force pressing the clutches together, the effective radius of the clutch pack, some friction coefficients, and finally the dependence on the differential speed. The choice of the differential speed function is to alleviate some of the computational complexities of zero crossings as the differential spends a significant portion of it's time near null differential speeds.

See Section 7.2.3 for how these are implemented within the vehicle simulator.

Sources:

Gadola, Marco, et al. "On the Passive Limited Slip Differential for High Performance Vehicle Applications." *Proceedings of the Advanced Vehicle Control Conference, Beijing, 16-20 July 2018.*

"Limited Slip Differential." *Mathworks Documentation,* 2020a, Mathworks, Inc., *https://www.mathworks.com/help/autoblks/ref/limitedslipdifferential.html*

Contributor	Date	Changes
Blake Christierson	3/20/20	First Draft

7.2.2 Semi-Empirical Motor Model

The main basis for this model is the speed-torque curve generated through a motor dynamometer test. By using the test data to characterize the maximum performance out of the motor-controller and motor combination given a supply voltage and current over a range of motor speeds. This data then needs to be scaled to the accumulator supply voltage and torque request. The motor torque is directly controlled and the required supply current is back calculated using the dynamometer data. The nomenclature for this section is quite extensive due to the amount of transformations applied to the data.

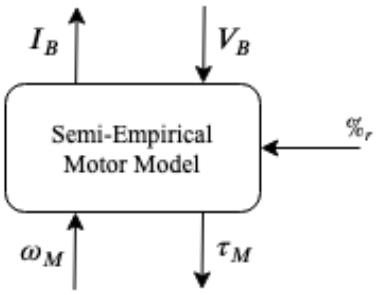

Figure 7.3: Semi-Empirical Motor Model Block Diagram

Symbol	Unit	Type	Description
$V_{B(Dyno)}$	V	Input	Battery Supply Voltage
$\omega_{M(Dyno)}$	$\frac{rad}{s}$	Input	Rotational Speed of Rotor
$\%_r$	[ ]	Input	Torque Request $\in [0, 1]$
$I_{B(Dyno)}$	A	Output	Battery Current Draw
$\tau_{M(Dyno)}$	Nm	Output	Output Motor Torque
$P_{B(Dyno)}$	kW	Output	Battery Power Supplied (Post)
$P_{M(Dyno)}$	kW	Output	Mechanical Power Output (Post)
$\eta_{(Dyno)}$	[ ]	State	System Efficiency

Table 7.3: Semi-Empirical Motor Model Nomenclature

The dynamometer provides the following data series:

$$V_{B(Dyno)} = V_{B(Dyno)}\left(\omega_{M(Dyno)}\right) \tag{7.2.10}$$
$$I_{B(Dyno)} = I_{B(Dyno)}\left(\omega_{M(Dyno)}\right) \tag{7.2.11}$$
$$\tau_{M(Dyno)} = \tau_{M(Dyno)}\left(\omega_{M(Dyno)}\right) \tag{7.2.12}$$
$$P_{B(Dyno)} = P_{B(Dyno)}\left(\omega_{M(Dyno)}\right) \tag{7.2.13}$$
$$P_{M(Dyno)} = P_{M(Dyno)}\left(\omega_{M(Dyno)}\right) \tag{7.2.14}$$
$$\eta_{(Dyno)} = \eta_{(Dyno)}\left(\omega_{M(Dyno)}\right) \tag{7.2.15}$$

The first transformation involves adjusting for the differing supply voltage between the dynamometer equipment and the accumulator. This scaling affects the argument

of each of the equations above by replacing $\omega_{M(Dyno)} \rightarrow \omega_M$. This is predominantly noticeable in the horizontal movement of the knee speed where the maximum torque available begins to decay. Note this makes V_B an input to the system.

$$\omega_M(V_B) = \frac{V_B}{V_{B(Dyno)}} \cdot \omega_{M(Dyno)} \tag{7.2.16}$$

Finally each of the functions except for the efficiency and supply voltage are scaled by the torque request giving the final following functions:

$$I_B = \%_r \cdot I_{B(Dyno)}\left(\omega_M(V_B)\right) \tag{7.2.17}$$
$$\tau_M = \%_r \cdot \tau_{M(Dyno)}\left(\omega_M(V_B)\right) \tag{7.2.18}$$
$$P_B = \%_r \cdot P_{B(Dyno)}\left(\omega_M(V_B)\right) \tag{7.2.19}$$
$$P_M = \%_r \cdot P_{M(Dyno)}\left(\omega_M(V_B)\right) \tag{7.2.20}$$
$$\eta = \eta_{(Dyno)}\left(\omega_M(V_B)\right) \tag{7.2.21}$$

There are more considerations for how the torque request is attenuated to avoid overtemp faults; however, that is discussed in the accumulator section. If that model is used, then the torque request here is replaced by the modulated torque request.

The implementation of this model involves parsing the dynamometer data, and then creating a Matlab custom function block within the powertrain model to do the scaling and then evaluate the model as a 3-d lookup table (in ω_M, V_B, & $\%_r$).

Sources:

Barham, Matt. *Design and Development of the Electrical Systems in an Electric Formula SAE Race Car* MS Thesis, University of Canterbury, Christchurch, New Zealand, 2017.

Contributor	Date	Changes
Blake Christierson	3/22/20	First Draft

7.2.3 Model Implementation

First, let's present the full set of pertinent equations that have been developed in this section. While most of the equations are directly transcribed, some of the efficiencies relating to the motor and chain have been slightly changed to align with the semi-empirical motor model that already takes efficiency into account. The slightly changed final nomenclature is also presented for clarity, the instances of Equation 3.1.1 are considered internal to the model to resolve the constrain equations imposed by the differential.

State Equation(s):

$$I_B = \%_r \cdot I_{B(Dyno)}\left(\omega_M(V_B)\right) \quad \text{(Revisited, 7.2.17)}$$

$$\tau_M = \%_r \cdot \tau_{M(Dyno)}\left(\omega_M(V_B)\right) \quad \text{(Revisited, 7.2.18)}$$

$$\dot{\omega}_M\left(J_M + \frac{J_D}{G_{FDR}}\right) + \omega_M\left(b_M + \frac{b_D}{G_{FDR}}\right) = \left(1 + \eta_C \cdot G_{FDR}\right)\tau_M - \tau_A \quad \text{(Modified, 7.2.5)}$$

$$\dot{\omega}_3 J_3 + \omega_3 b_3 = \eta_D \tau_3 - F_{x,3} r_e - F_{b,3} r_r \quad \text{(Revisited, 3.1.1)}$$

$$\dot{\omega}_4 J_4 + \omega_4 b_4 = \eta_D \tau_4 - F_{x,4} r_e - F_{b,4} r_r \quad \text{(Revisited, 3.1.1)}$$

Constraint Equation(s):

$$\begin{cases} \omega_M = G_{FDR} \cdot \omega_3 = G_{FDR} \cdot \omega_4, & \text{if } \tau_A \in [\tau_B, \tau_D] \\ \omega_M = \frac{G_{FDR}}{2}\left(\omega_3 + \omega_4\right), & \text{otherwise} \end{cases} \quad \text{(From, 7.2.4 \& 7.2.6)}$$

$$\begin{cases} \tau_A \cdot G_{FDR} = \tau_3 + \tau_4, & \text{if } \tau_A \in [\tau_B, \tau_D] \\ \begin{cases} \tau_3 = \frac{G_{FDR}}{2} \cdot \tau_A - \operatorname{sgn}\left(\Delta\omega\right) \cdot \Delta\tau \\ \tau_4 = \frac{G_{FDR}}{2} \cdot \tau_A + \operatorname{sgn}\left(\Delta\omega\right) \cdot \Delta\tau \end{cases}, & \text{otherwise} \end{cases} \quad \text{(From, 7.2.3 \& 7.2.7)}$$

Evaluation Equation(s):

$$\omega_M(V_B) = \frac{V_B}{V_{B(Dyno)}} \cdot \omega_{M(Dyno)} \quad \text{(Revisited, 7.2.16)}$$

$$P_B = \%_r \cdot P_{B(Dyno)}\left(\omega_M(V_B)\right) \quad \text{(Revisited, 7.2.19)}$$

$$\eta = \eta_{(Dyno)}\left(\omega_M(V_B)\right) \quad \text{(Revisited, 7.2.21)}$$

$$\Delta\omega = \omega_3 - \omega_4 \quad \text{(Revisited, 7.2.8)}$$

$$\Delta\tau = \left(\frac{\tau_A \cdot G_{FDR}}{r_{Ramp}} \cdot \cot\left(\sigma_{D,B}\right)\right)\left(\frac{2}{3} \cdot \frac{r_o^3 - r_i^3}{r_o^2 - r_i^2}\right)\left(\mu_c N\right)\left(|\Delta\omega| \cdot \tanh\left(4|\Delta\omega|\right)\right) \quad \text{(From, 7.2.3 \& 7.2.9)}$$

There are four degrees of freedom in the system: ω_M, ω_3, ω_4, τ_A, and the three state equations and solitary constraint provide a properly constrained DAE system. The scheme will be to solve for the derivative of the velocity for each state equation and then use an algebraic constraint block to solve for the total torque applied to the axle at each time step iteratively. This is not the most efficient implementation, and should be revisited as it makes the model quite computationally intensive.

Symbol	Unit	Type	Description
V_B	V	Input	Battery Supply Voltage
$\%_r$	[ ]	Input	Torque Request $\in [0, 1]$
$\omega_{3,4}$	$\frac{rad}{s}$	Input	Rear Left & Right Wheel Speeds
I_B	A	Output	Battery Current Draw
P_B	kW	Output	Battery Power Supplied
η_M	[ ]	Output	Motor Controller & Motor System Efficiency
$\tau_{3,4}$	Nm	Output	Rear Left & Right Axle Drive Torques
τ_M	Nm	Variable	Motor Torque
ω_M	$\frac{rad}{s}$	Variable	Rotational Speed of Rotor
τ_A	Nm	Variable	Total Axle Drive Torque
$\Delta\tau$	Nm	Variable	Differential Torque
$\Delta\omega$	$\frac{rad}{s}$	Variable	Differential Torque
η_D	[ ]	Variable	Differential Efficiency
G_{FDR}	[ ]	Parameter	Final Drive Ratio (Gearing Ratio)
η_C	[ ]	Parameter	Chain Drive Efficiency
$\sigma_{D,B}$	deg	Parameter	Drive & Brake Ramp Angles
$\tau_{D,B}$	Nm	Parameter	Drive & Brake Preload
J_M	kgm^2	Constant	Rotational Inertia of Motor
J_D	kgm^2	Constant	Rotational Inertia of Differential & Sprassy
b_M	Nms	Constant	Rotational Dampening of Motor
b_D	Nms	Constant	Rotational Dampening of Differential
r_{Ramp}	m	Constant	Ramp Radius
r_o	m	Constant	Outer Radius of Clutch Packs
r_i	m	Constant	Inner Radius of Clutch Pack
μ_c	[ ]	Constant	Clutch Coefficient of Friction
N	[ ]	Constant	Number of Friction Surfaces

Table 7.4: Complete Medium Fidelity Powertrain Model Nomenclature

7.3 Dynamic Accumulator Bond Graph Models

$$f_1 = f_2 + f_{13}$$
$$e_1 = e_2 = e_3$$

$$f_2 = f_3 + f_4$$

Chapter 8

Controllers & Driver Models